

Dynamic properties of simple liquids: Dependence on the softness of the potential core

N. Anento, J. A. Padró, and M. Canales

Citation: *The Journal of Chemical Physics* **111**, 10210 (1999); doi: 10.1063/1.480371

View online: <http://dx.doi.org/10.1063/1.480371>

View Table of Contents: <http://scitation.aip.org/content/aip/journal/jcp/111/22?ver=pdfcov>

Published by the [AIP Publishing](#)

Articles you may be interested in

[Effect of softness of the potential on the stress anisotropy in liquids](#)

J. Chem. Phys. **126**, 224511 (2007); 10.1063/1.2738475

[The influence of potential softness on the transport coefficients of simple fluids](#)

J. Chem. Phys. **122**, 234504 (2005); 10.1063/1.1931668

[Particle packing in soft- and hard-potential liquids](#)

J. Chem. Phys. **119**, 9667 (2003); 10.1063/1.1615962

[Molecular dynamics simulations of simple dipolar liquids in spherical cavity: Effects of confinement on structural, dielectric, and dynamical properties](#)

J. Chem. Phys. **111**, 1223 (1999); 10.1063/1.479307

[The effects of pressure on structural and dynamical properties of associated liquids: Molecular dynamics calculations for the extended simple point charge model of water](#)

J. Chem. Phys. **107**, 8561 (1997); 10.1063/1.475162



Dynamic properties of simple liquids: Dependence on the softness of the potential core

N. Anento and J. A. Padró

Departament de Física Fonamental, Universitat de Barcelona, Diagonal, 647, 08028 Barcelona, Spain

M. Canales

Departament de Física i Enginyeria Nuclear, Universitat Politècnica de Catalunya, Camput Nord. Sor Eulàlia d'Anzizu, B4-B5, 08034 Barcelona, Spain

(Received 13 May 1999; accepted 14 September 1999)

The dependence of both individual and collective dynamic properties of simple liquids on the steepness of the potential cores is analyzed. Molecular dynamics simulations of liquids in identical conditions but assuming two repulsive interaction potentials with very different softness have been carried out. Two liquids at very different densities (with volume packing fractions $\eta=0.5$ and $\eta=0.3$) have been considered for each potential. The study of the dynamic collective properties includes the dynamic structure factor and the longitudinal and transverse current correlations. It has been corroborated that longitudinal modes associated with density fluctuations propagate up to higher wave numbers in liquids with softer potential cores. However, the propagating transversal modes in dense liquids are weakly influenced by the hardness of the potential core. Other properties such as the sound velocity in liquids at high density or the dynamic structure factor at the kinetic regime are rather insensitive to the details of the repulsive interactions. The velocity correlation functions for liquids with soft repulsive potential walls are markedly oscillatory. These oscillations are associated with the coupling of the atomic velocity to collective density fluctuations. © 1999 American Institute of Physics. [S0021-9606(99)51046-5]

I. INTRODUCTION

Molecular dynamics (MD) simulation is a very useful tool to study the microscopic properties of liquids. This technique, which is based on the assumption of an interaction potential model, not only allows us to simulate realistic systems but also to perform computer experiments of ideal systems with interaction potentials deliberately modeled to analyze specific problems. These ideal computer experiments can be applied to investigate the relationship between the characteristics of a given interaction potential and the properties of the corresponding system. This kind of information is very helpful for a deeper understanding of the basis of the behavior of liquids and a useful guide for the improvement of the potentials for real systems.

It is well established that the short-range repulsive interatomic forces essentially determine both the structure and single atomic motions in dense liquids. This is the basis of the perturbation theories that have been successfully applied to the calculation of the structure and thermodynamic properties of fluids.¹ Moreover, the repulsive potential core plays a key role on the dynamic properties of a liquid. The large differences between the collective dynamic properties of liquid alkali metals and rare gas liquids have been attributed to the softer potential cores of the former.^{2,3} So, although the influence of the attractive forces may be important at certain thermodynamic conditions,⁴⁻⁶ the steepness of the repulsive core is a very significant feature of the intermolecular potentials for simple liquids.

The dependence of both individual and collective dynamic properties of simple liquids on the hardness of their

repulsive potential cores is investigated in this work. The study is based on the comparison of the properties resulting from MD simulations of two systems at the same conditions but assuming two repulsive potentials with very different softness. On the one hand, we have considered a 6th-inverse-power potential. This potential is softer than the core of the potentials usually assumed for liquid alkali metals,⁵⁻⁸ although potentials of similar softness have been proposed for other liquid metals such as the Li₄Pb alloy.^{9,10} Due to the appearance of well-defined high-frequency density excitations that were associated with a “fast sound mode” propagating through the light atoms,¹⁰ the dynamic collective properties of this alloy have recently been the subject of several studies.¹¹ On the other hand, we have considered the repulsive wall of a Lennard-Jones (LJ) potential. It should be noted that this core is harder than that of a 12th-inverse-power potential with the same σ due to the attractive contribution of the r^{-6} term in the LJ potential. In order to discuss the possible dependence of the results on the degree of close packing of the atoms in the liquid we have simulated two systems at very different densities for each potential model.

II. COMPUTER SIMULATIONS

We carried out MD simulations of systems made up to 864 particles with the mass of Ar ($m=39.95$ uma) enclosed in a box with ordinary periodic boundary conditions. The temperature was $T=120$ K in all the simulations. MD runs of $\approx 10^5$ time steps with an integration time step of 10 fs were performed for each system. Several dynamic properties were determined from the configurations generated during these

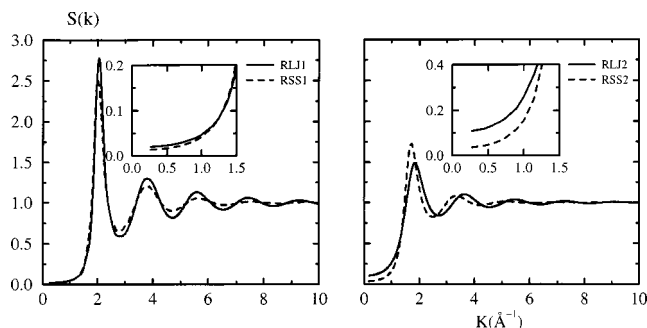


FIG. 1. Structure factors of the simulated systems. The insets show the low k -behaviors at larger scales.

runs according to the usual definitions.^{3,12} The study includes the velocity autocorrelation function $[C(t)]$, the intermediate scattering function $[F_S(k, t), F(k, t)]$ and both the longitudinal and the transverse current correlation functions $[C_L(k, t), C_T(k, t)]$. The frequency-dependent spectra $[C(\omega), S(k, \omega), C_L(k, \omega), C_T(k, \omega)]$ were obtained by Fourier transforming the corresponding time-dependent correlation functions. $C_L(k, \omega)$ was also determined by using the equation^{3,9} $C_L(k, \omega) = \omega^2 S(k, \omega)$. The resulting $C_L(k, \omega)$ s were in satisfactory accordance with those directly obtained as the Fourier transforms of the $C_L(k, t)$ s. The k -dependent properties were calculated for ≈ 20 wave numbers, ranging from $k = 0.27 \text{ \AA}^{-1}$ to $k = 4.4 \text{ \AA}^{-1}$, compatible with the periodic boundary conditions.

Two repulsive potentials were assumed:

RLJ: a LJ potential with the usual parameters for liquid Ar ($\sigma = 3.405 \text{ \AA}$; $\epsilon = 119.8 k_B$) but truncated at the position of its first minimum ($r_c = 2^{1/6}\sigma$);

RSS: a soft sphere 6th-inverse-power potential ($V(r) \propto (\sigma/r)^6$) with the same σ than RLJ (in this case the interactions were truncated at 2.5σ).

It should be emphasized that RSS is markedly softer than RLJ. We have estimated that the softness of RLJ is approximately equivalent to an inverse-power potential with $n \approx 16$ – 20 . For each interaction potential we carried out MD simulations at two particle densities, i.e., $\rho_1 = 0.024 \text{ \AA}^{-3}$ and $\rho_2 = 0.014 \text{ \AA}^{-3}$. The corresponding volume packing fractions ($\eta \equiv \rho \pi \sigma^3/6$) are $\eta_1 = 0.5$ and $\eta_2 = 0.3$, respectively. These densities are somewhat higher than those of the critical point and the triple point of Ar, respectively, and the temperature is intermediate between those of these two points. The MD runs at the higher density will be termed RLJ1 and RSS1, whereas those at the lower density will be termed RLJ2 and RSS2.

The structure factors $S(k)$ for the four simulated liquids were determined from the radial distribution functions obtained during the MD configurations. The results are represented in Fig. 1. As could be expected, the structure of the systems at different densities shows large differences whereas the discrepancies due to the interaction potentials are smaller and mainly reflected on the height of the $S(k)$ peaks. The positions of the peaks for RLJ1 and RSS1 are very close whereas little differences in the location of the

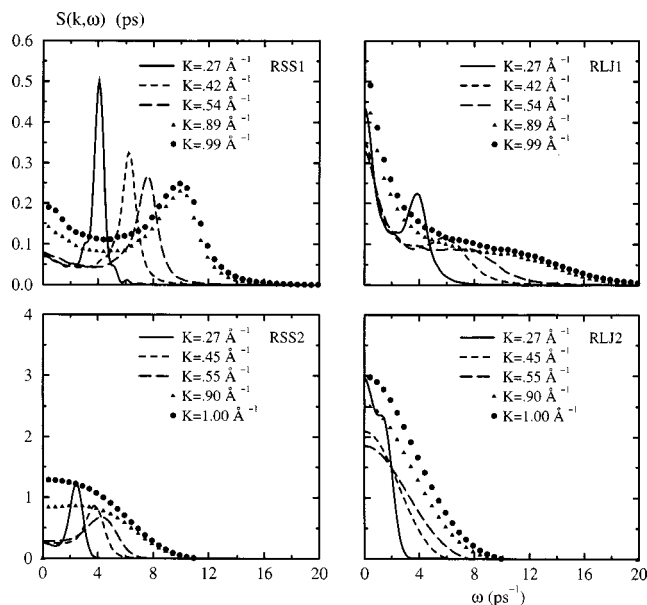


FIG. 2. Dynamic structure factors.

$S(k)$ maxima and minima may be observed for the system at lower density.

III. COLLECTIVE PROPERTIES

The dynamic structure factor $[S(k, \omega)]$ is a basic quantity to study the dynamics of density fluctuations in liquids. At long wavelengths (hydrodynamic regime), $S(k, \omega)$ for a given k consists of a Rayleigh peak at $\omega = 0$ and two shifted Brillouin peaks which are associated with the propagation of longitudinal modes analogous to the acoustic phonons in solids.³ We found that $S(k, \omega)$ shows a hydrodynamiclike structure for all the simulated systems but the range of wavelengths for which the Brillouin peaks are visible is very different (Fig. 2). For RSS1, the Brillouin peak is well defined up to $k \approx 1.4 \text{ \AA}^{-1}$, whereas it broadens into a shoulder at higher k -values. For RLJ1, the Brillouin peak can be noticed up to $k \approx 0.6 \text{ \AA}^{-1}$. For the liquids at low density the Brillouin peak disappears at lower wave numbers, i.e., at $k \approx 0.9 \text{ \AA}^{-1}$ for RSS2, whereas for RLJ2 only can be observed for the smallest k ($k = 0.27 \text{ \AA}^{-1}$). According to the results for LJ fluids and liquid metals,^{2–6} the softer is the potential core, the wider is the wavelength interval with noticeable $S(k, \omega)$ Brillouin peaks. Moreover, this interval becomes larger as density increases. It should be pointed out that the height of the Brillouin peak relative to the central Rayleigh peak is markedly smaller for the harder potential, which is consistent with recent MD studies of different dense liquids^{5,6} as well as with the predictions of the viscoelastic theory.^{3,12,13}

The shape of the $S(k, \omega)$ curves for a given k approaches to a Gaussian as the wavenumber increases (kinetic regime) and for k -values around the maximum of the static structure factor ($k \approx 2 \text{ \AA}^{-1}$ for RSS1 and RLJ1, $k \approx 1.75 \text{ \AA}^{-1}$ for RSS2 and RLJ2) the Rayleigh peak becomes very high and narrow (de Gennes narrowing).³ For each system, there is an intermediate interval of k s for which $S(k, \omega)$ does not present a well-defined Brillouin peak but shows a shoulder. The

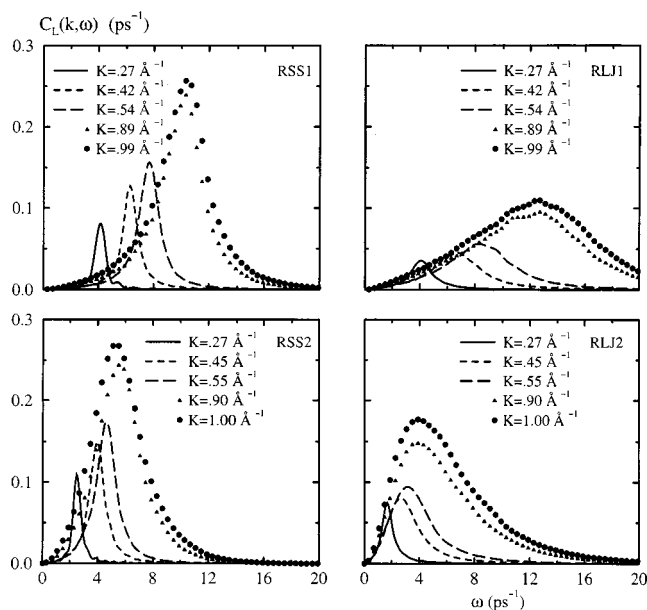


FIG. 3. Longitudinal current spectra.

minimum wave number for which $S(k, \omega)$ shows a monotonous decay goes from $k \approx 1.7 \text{ \AA}^{-1}$ for RSS1 to $k \approx 0.9 \text{ \AA}^{-1}$ for RLJ2 (Fig. 2). The influence of the potential hardness is rather small beyond the hydrodynamic regime and after the de Gennes narrowing the difference between the monotonous decays of the $S(k, \omega)$ s for the systems at the same density but different potential core are almost undiscernible.

In the hydrodynamic limit ($k \rightarrow 0$), the relation between the frequency and the wave number of the Brillouin peak gives the adiabatic sound velocity.^{3,12,14} Alternatively, this velocity may be estimated from the positions of the maxima of the $C_L(k, \omega)$ spectra.¹⁴ Thus, the dispersion relation curves can be determined for all the systems since $C_L(k, \omega)$ shows a maximum at any k (Fig. 3). The $C_L(k, \omega)$ peaks for RLJ1 and RSS1 at low k s are located at similar positions (Fig. 3) and the initial slopes of the dispersion curves for these two systems do not show significant differences (Fig. 4). This shows that the velocity of propagation of the longitudinal modes in dense liquids is little influenced by the steepness of the potential core. However, the influence of the softness of the potential core on the sound velocity becomes more marked for liquids at lower density. In these conditions, the softer is the potential the faster is the propagation of longitudinal modes. For RSS2 and RLJ2 the positions of the $C_L(k, \omega)$ peaks change very slowly with k and the velocity of the soundwaves is rather small for these systems.

It is interesting to analyze the behavior of $S(k)$ in the limit $k \rightarrow 0$, since $S(0)$ is proportional to the isothermal compressibility of the liquid. However, the $S(k)$ functions at low k -values could not be calculated by Fourier transforming the radial distributions functions because they were only determined for a limit r -interval. We have then used the relation $S(k) = F(k, 0)$. The $S(k)$ functions in the insets of Fig. 1 corroborate that the isothermal compressibility becomes lower as density increases. Moreover, in dense liquids the

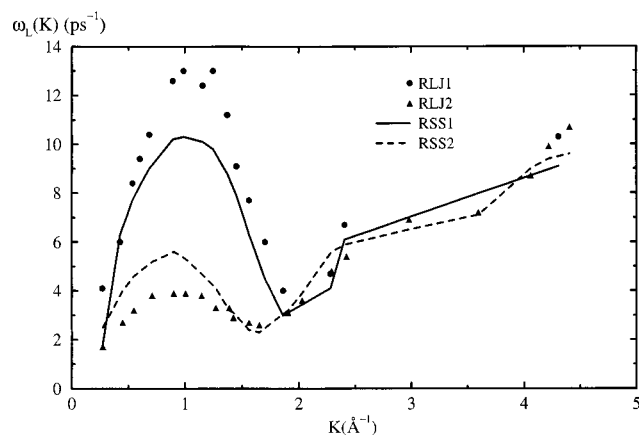


FIG. 4. Dispersion curves obtained from the peaks of the longitudinal current spectra.

value of $S(0)$ is almost independent on the details of the repulsive interactions whereas in the liquids at lower density the influence of the softness of the potential core is more marked (the compressibility for RLJ2 is higher than for RSS2). The low compressibility of the liquids at the state 1 indicates that the atoms in these systems are very close packed. On the contrary, the interatomic distances in the liquids at the state 2 are somewhat greater, and then the characteristics of the potential wall have a more relevant influence. The $S(0)$ results are consistent with the sound velocity findings. There are no significant differences in both the sound velocity and the isothermal compressibility of the RLJ1 and RSS1 systems whereas at the state 2 the sound velocity is higher for the less compressible liquid.

The spectra of the transverse current correlation functions for several k s are shown in Fig. 5. It is well known that, at certain wave numbers, $C_T(k, \omega)$ can show a peak at non-zero frequencies that reflects the propagation of transverse current fluctuations (shear waves) through the liquid. The

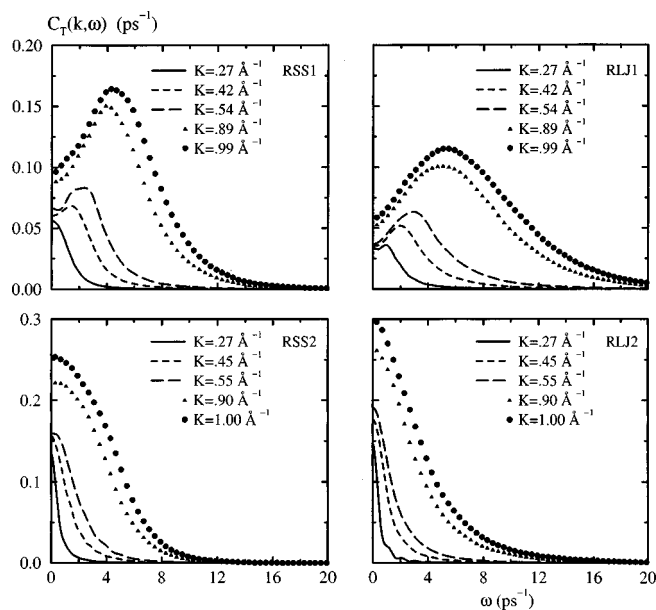


FIG. 5. Transverse current spectra.

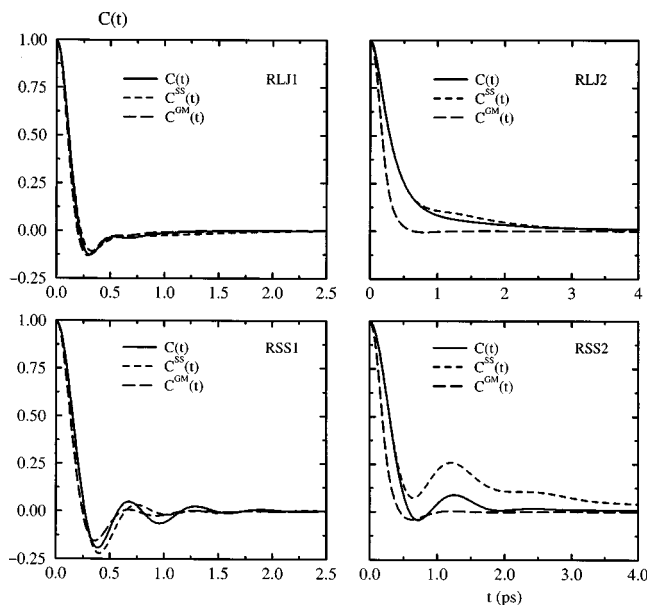


FIG. 6. Normalized velocity autocorrelation functions directly obtained from MD simulations [$C(t)$] and calculated according to theoretical approaches [$C^{GM}(t)$, $C^{SS}(t)$].

$C_T(k, \omega)$ functions in the systems at high density present this peak for rather wide k -intervals. In the case of RLJ1 and RSS1 the $C_T(k, \omega)$ maximum may be observed for all the considered wave numbers, except for the lowest ($K = 0.27 \text{ \AA}^{-1}$) in the case of RSS1. On the contrary, the $C_T(k, \omega)$ functions for RLJ2 and RSS2 do not show any noticeable maximum within the considered wavelength intervals. This indicates that transverse current fluctuations in liquids at low density are mainly dissipated by diffusive processes and propagating shear modes (if they exist) cannot be distinguished in the $C_T(k, \omega)$ functions. According to these findings, the range of wavelengths over which propagating shear modes may be observed in the $C_T(k, \omega)$ spectrum is markedly dependent on the density of the system, which suggests that these modes cannot propagate when the atoms are not very close packed. Unlike for longitudinal modes, the propagation of shear waves is little influenced by the softness of the potential core.

IV. VELOCITY AUTOCORRELATION FUNCTION

The $C(t)$ function is the property ordinarily used for the study of the dynamic behavior of single atoms in short time scales. However, this behavior is largely influenced by the coupling of the individual atomic motions to the collective modes in the liquid. The relation between the collective modes and $C(t)$ functions is discussed in this section. The $C(t)$ function for RLJ1 shows a deep minimum with negative values (backscattering) followed by a shoulder (Fig. 6). This negative minimum, which is typical of the $C(t)$ for dense liquids, reflects a high probability of large deflections in the collisions of the atom with their neighbors. For RLJ2, the $C(t)$ function shows the monotonous exponential-like decay characteristic of liquids at low density. Unlike for ordinary LJ and RLJ liquids, the $C(t)$ functions for the two RSS systems show marked oscillations after the first mini-

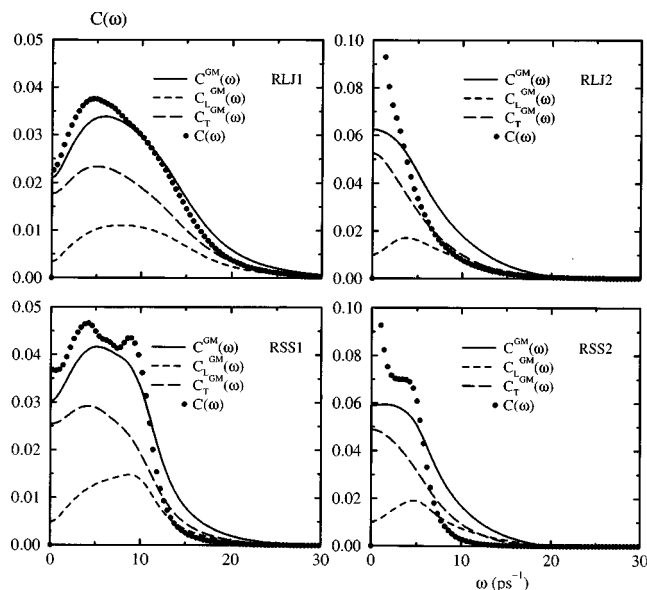


FIG. 7. Power spectra of the velocity autocorrelation functions and the longitudinal and transverse contributions calculated according to the GM theoretical approach.

mum that are wider and more persistent for the system at higher density. Moreover, the $C(t)$ for RSS1 show a slower initial decay (higher backscattering time) and a more pronounced minimum (deeper backscattering) than that for RLJ1. These differences, which are consistent with earlier findings by Wijeyesekera and Kushick,¹⁵ should be attributed to the softer core of the former potential. The marked negative values of the first $C(t)$ minima for RSS1 and RSS2 reflect a rather high degree of coherence between different backscattering events.¹⁵ This fact, together with the pronounced oscillations after minimum, indicate that molecular collisions in these systems should be correlated and the effect of these correlations increases with the softness of the potential core.

The spectra of the $C(t)$ functions [$C(\omega)$] are shown in Fig. 7. The $C(\omega)$ curves for both RSS1 and RLJ1 show a first maximum (at $\omega_{\max} \approx 4 \text{ ps}^{-1}$ and $\omega_{\max} \approx 4.7 \text{ ps}^{-1}$, respectively) that does not appear in the corresponding $C(\omega)$ s for liquids at state 2. This maximum has been associated with the atomic oscillations due to the collisions of a tagged atom with their neighbors (cage effects). Such oscillatory motions are enhanced in dense liquids, where atoms are highly close packed. Besides, the $C(\omega)$ functions for the soft potential cores show a second peak (at $\omega_{\max} \approx 9 \text{ ps}^{-1}$) in the case of RSS1 and a shoulder ($\omega_{\max} \approx 3 \text{ ps}^{-1}$) in the case of RLJ1 which cannot be observed the $C(\omega)$ s for the corresponding RLJ systems. These $C(\omega)$ features are the result of the marked oscillations of the $C(t)$ functions after their first minimum. Consistently with the wavelength of the $C(t)$ oscillations (Fig. 6), the frequencies corresponding to the RSS1 peak are higher than those corresponding to the RSS2 peak. These results are in accordance with those from the MD study for dense soft sphere liquids by Kambayashi and Hiwatari,¹³ where also was found a side $C(\omega)$ peak that becomes more marked as the potential is softer. This side peak was ascribed to the coupling of the motions of single

particles with the collective density fluctuations in the liquid. Recently, it has also been observed the presence of an incipient side peak in the $C(\omega)$ spectrum for liquid Li close to the triple point,⁶ which according to the findings discussed in this section should be associated with the rather soft repulsive core of the effective interatomic potential for Li.

The initial values of $C(\omega)$ are proportional to the self-diffusion coefficients D .^{3,12,14} The initial $C(\omega)$ -value for RSS1 is almost twice than that for RLJ1, whereas the initial $C(\omega)$ -value for RSS2 is notoriously lower than that for RLJ2. This shows that there is no significant correlation between the softness of the potential and the values of the D coefficients. It should be noted that the self-diffusion coefficients for RSS1 and RSS2 are of the same order of magnitude than those for RLJ1 and RLJ2, respectively. This corroborates that despite the solidlike shape of the $C(t)$ functions the RSS systems are liquids.

The behavior of the $C(t)$ functions has been first analyzed by considering the theoretical approach by Gaskell and Miller,¹⁶ which is one of the simplest applications of the mode coupling concepts to the study of the dynamic properties of dense liquids. This approach, which is a generalization of the hydrodynamic description of the fluid to the microscopic scales, was successfully applied to the $C(t)$ functions for both LJ and alkali-metal liquids^{16,17} and, more recently, for the molecular center-of-mass of liquid water.¹⁸ The theory is based on the introduction of a microscopic velocity field

$$\mathbf{v}(\mathbf{r}, t) = \sum_j f(|\mathbf{r} - \mathbf{r}_j(t)|) \mathbf{v}_j(t), \quad (1)$$

where $f(r)$ is a form factor that may be determined by taking into account that the velocity field around the position of an atom should be very close to the actual velocity of this atom. Gaskell and Miller obtained an expression that allows us to calculate the velocity correlation functions ($C^{\text{GM}}(t)$) from the longitudinal and transversal current correlation functions^{12,16}

$$C^{\text{GM}}(t) = (24\pi k_B T m)^{-1} \times \int f(k) [C_L(k, t) + 2C_T(k, t)] F_S(k, t) d\mathbf{k}, \quad (2)$$

where $f(k)$ is the Fourier transform of $f(r)$. We calculated the $C^{\text{GM}}(t)$ functions for the four systems analyzed in this work. This calculation was carried out by using the dynamic collective properties [$F_S(k, t)$, $C_L(k, t)$, and $C_T(k, t)$] obtained during the MD simulations. The assumed form factor was $f(r) = \exp[-(r/a)^{12}]$, where a is an effective radius determined from the number density (n) of the liquid according to the relation $4\pi n a^3/3 = 1$.¹⁶ It should be pointed out that the calculation of $C^{\text{GM}}(t)$ requires a numerical integration over k but the k -dependent dynamic properties were only determined between $k = 0.27 \text{ \AA}^{-1}$ to $k = 4.4 \text{ \AA}^{-1}$. For the sake of the $f(k)$ characteristics the contributions to $C^{\text{GM}}(t)$ corresponding to wave numbers beyond this interval are not significant but the finite number of considered k s did not allow us an accurate determination of $C^{\text{GM}}(t)$. Nevertheless,

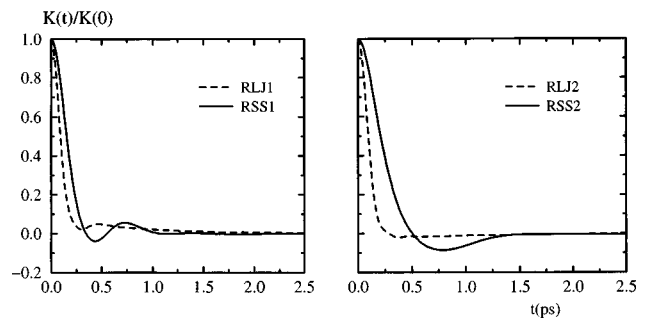


FIG. 8. Normalized memory functions for the velocity autocorrelation functions obtained from the MD simulations.

the numerical inaccuracies should not affect our conclusions, which are mainly based on the qualitative trends of the $C^{\text{GM}}(t)$ functions.

The four $C^{\text{GM}}(t)$ s are compared with the “exact” $C(t)$ s directly obtained during the MD simulations in Fig. 6. For the systems at high density the accordance is quite good, especially in the case of RLJ1. Despite little discrepancies, $C^{\text{GM}}(t)$ qualitatively reproduces the oscillatory behavior of the $C(t)$ for RSS1. On the contrary, large disagreements between $C^{\text{GM}}(t)$ and $C(t)$ may be observed for the RSS2 and RLJ2 systems. This shows that the basic assumptions of the GM theory are not fulfilled at the density of these systems. It should be noted that this theory was proposed for liquids at high density and successfully checked for dense LJ and alkali metal in liquid state.^{16,17}

One of the main advantages of the Gaskell and Miller approximation is that it allows us to split the $C(t)$ functions into longitudinal and transverse contributions [see Eq. (2)]. This decomposition can also be translated to the corresponding $C(\omega)$ spectra. Thus, despite the noticeable discrepancies between $C^{\text{GM}}(\omega)$ and $C(\omega)$, valuable information on the relative contributions of the longitudinal [$C_L^{\text{GM}}(\omega)$] and transverse [$C_T^{\text{GM}}(\omega)$] terms to $C(\omega)$ may be obtained (Fig. 7). The low-frequency maximum in the $C(\omega)$ spectra of dense liquids should be associated with the transverse current contribution whereas the other peak (or shoulder) in the $C(\omega)$ s for soft-core potentials should be attributed to the longitudinal current. Since $C(\omega)$ at low frequencies is dominated by the transverse modes, the contribution of the longitudinal modes to the diffusion coefficient is rather small. These findings are in agreement with earlier results for LJ and liquid argon and liquid sodium.¹⁷

A more basic quantity, called memory function [$K(t)$], is frequently used in theoretical analyses of the $C(t)$ function. $K(t)$ is related to $C(t)$ through a Volterra-type integral equation^{3,12,14}

$$\dot{C}(t) = - \int_0^t K(t') C(t-t') dt'. \quad (3)$$

We determined the $K(t)$ s for the four systems by numerical integration of this equation.¹⁹ As with $C(t)$ s, the resulting $K(t)$ functions have a marked dependence on the softness of the potential core. The $K(t)$ curves for the RSS potential show slower decays and more pronounced minima than the ones for RLJ at the same density (Fig. 8). Moreover, notice-

able oscillations after the first $K(t)$ minimum may be observed in the case of RSS1, though for RSS2 the oscillations are very damped.

The most usual theoretical approaches to the memory function in liquids are based on the mode-coupling theories.^{12,14} One of the most successful applications of these theories is that proposed by Sjögren and Sjölander.²⁰ These authors assumed that the memory function could be divided into two terms,

$$K^{\text{SS}}(t) = K_B(t) + K_{\text{MC}}(t), \quad (4)$$

where $K_B(t)$ is attributed to binary collisions and $K_{\text{MC}}(t)$ is associated with collective effects. According to the mode-coupling ideas, Sjögren and Sjölander obtained an analytical expression for $K_{\text{MC}}(t)$, which is the result of four contributions,

$$K_{\text{MC}}(t) = K_{00}(t) + K_{01}(t) + K_{11}(t) + K_{22}(t), \quad (5)$$

$K_{00}(t)$ incorporates the effects of the coupling of the velocity of a tagged particle with the density fluctuations of the surrounding medium. $K_{01}(t)$ reflects the coupling with the first derivative of the dynamic structure factor. The $K_{11}(t)$ and $K_{22}(t)$ terms are attributed to the coupling with the longitudinal and the transverse currents, respectively. These four terms may be calculated from different dynamical quantities,^{20,21} including $F(k, t)$, $F_s(k, t)$, $C_L(k, t)$, and $C_T(k, t)$.

We determined $K_{ij}(t)$ and $K_{\text{MC}}(t)$ for the four systems by using the dynamic collective properties obtained from the MD simulations (details about the numerical procedure used for this calculation are given in Ref. 21). It was assumed that $K_B(t)$ is a Gaussian function $K_B(t) = \Omega_0^2 \exp(-t^2/\tau^2)$, where Ω_0^2 is the Einstein frequency and τ is a parameter that was determined by fitting $K_B(t)$ to the $K(t) - K_{\text{MC}}(t)$ values. The $C^{\text{SS}}(t)$ functions corresponding to the $K^{\text{SS}}(t)$ memory functions obtained from $K_B(t)$ and $K_{\text{MC}}(t)$ were calculated by numerically solving Eq. (3) according to the procedure described elsewhere.¹⁹ $C^{\text{SS}}(t)$ and $C(t)$ are very close for RLJ1 whereas they show some discrepancies for RLJ2 and RSS1 (Fig. 6). For RSS2 the discrepancies are larger but $C^{\text{SS}}(t)$ qualitatively reproduces the $C(t)$ oscillations for this system. In general, the agreement of $C^{\text{SS}}(t)$ with the corresponding $C(t)$ is quite good and better than in the case of $C^{\text{GM}}(t)$. Nevertheless, it should be pointed out that the binary contribution to $C^{\text{SS}}(t)$ was not independently determined but fitted to a set of values obtained from the $K(t)$ function resulting from the MD simulations. When other theoretical approximations to $K_B(t)$ are used, the agreement between $C^{\text{SS}}(t)$ and $C(t)$ is somewhat worse.²¹ The failure of the MC theory of Sjögren and Sjölander for an accurate calculation of the $C(t)$ functions for certain liquids was attributed to a breakdown of one of the basic assumptions, the decomposition of the memory function into two independent terms.^{21,22}

The resulting $K_{ij}(t)$ functions are shown in Fig. 9. It should be pointed out that these functions could not be accurately determined since their calculation requires a numerical integration over k of quantities that were only determined

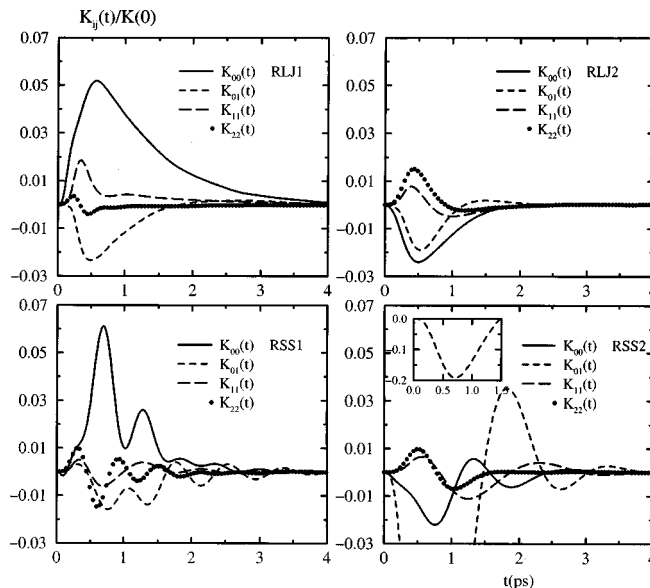


FIG. 9. Mode coupling contributions to the memory function determined according to the SS approach.

for a finite number of wavenumbers. However, the qualitative trends of the $K_{ij}(t)$ functions resulting from these calculations using MD data can provide us with more realistic information for a given system than $K_{ij}(t)$ functions obtained in other studies from general theoretical approximations. The $K_{ij}(t)$ functions corresponding to the RSS potential show marked oscillations that are not observed for RLJ. As with other properties analyzed in this paper, this fact must be associated with the softness of the RSS potential. This is also consistent with the more oscillatory $K_{ij}(t)$ s for metal liquids as compared with those for LJ liquids in analogous conditions.²¹

The results for RLJ1 are similar to those for other dense liquids.^{12,21} The largest contribution to $K_{\text{MC}}(t)$ is $K_{00}(t)$ and there is a significant cancellation of the $K_{01}(t)$ and $K_{11}(t)$ contributions. For RSS1, the most important contribution is also $K_{00}(t)$ but both $K_{01}(t)$ and $K_{11}(t)$ are negative and there is not cancellation between them. The results for the systems at low density are very different. $K_{00}(t)$ is negative and of similar magnitude to the other $K_{ij}(t)$ s. However, $K_{01}(t)$ for RSS2 is markedly larger than the other three $K_{ij}(t)$ s for this system (see the inset in Fig. 9). We have checked that these large $K_{01}(t)$ -values produce the oscillatory behavior of the $C^{\text{SS}}(t)$ function for this system. The prevalence of both $K_{00}(t)$ in the case of RSS1 and $K_{01}(t)$ in the case of RSS2 are consistent with the attribution of the $C(t)$ oscillations and the corresponding second “high-frequency” $C(\omega)$ maximum to the coupling of the atom’s velocity with the density fluctuations. The $K_{22}(t)$ term is very small for RLJ1 whereas for the other systems it is also small but of similar magnitude to other $K_{ij}(t)$ terms. It should be pointed out that the $K^{\text{SS}}(t)$ functions are largely dominated by the $K_B(t)$ term.²¹ So, the different $K_{ij}(t)$ contributions to $C^{\text{SS}}(t)$ cannot be directly compared with the contributions of the longitudinal and transverse currents to the $C^{\text{GM}}(t)$ functions previously analyzed in this section.

V. CONCLUDING REMARKS

The results obtained in this study have corroborated that the differences in the collective dynamic properties of liquid metals and rare gas liquids^{2,3} should be attributed to the softer repulsive walls of the potentials for the former systems. The dynamic structure factor show Brillouin peaks that persist up to larger wave numbers at higher density, being this persistence notoriously larger as the potential core is softer. This finding suggests that interatomic collisions through hard cores do not favor the coherence of the atomic motions that is required for the propagation of the longitudinal modes associated with density fluctuations. On the contrary, the presence of visible peaks in the transverse current spectra is mainly dependent on the density of the liquid and is not very sensitive to the hardness of the potential core. This should be associated with the different nature of the transverse modes, being the ability of liquids to sustain propagating shear waves mainly related to the close packing of atoms in the liquid. It should be noted that the dynamic structure factor at high ks (kinetic regime) is not sensitive to the details of the repulsive interactions. The velocity of the sound waves in dense liquids is also rather insensitive to the hardness of the soft core potential.

The velocity autocorrelation functions for liquids with soft potential cores show marked oscillations that are also reflected in the corresponding memory functions and power spectra. The peak (or shoulder) induced by these oscillations on the power spectra, has been attributed to the coupling of the atomic velocity of the density fluctuations of the surrounding fluid. This is consistent with the observed enhancement of longitudinal modes for soft potential cores. The first maximum in the power spectra, which is characteristic of dense liquids, is related to the transverse currents. This is in accordance with the observed relationship between shear modes and the atomic close packing.

ACKNOWLEDGMENTS

Financial support of DGICYT (Grant No. PB96-0170-C03) and CIRIT (Grant No. GRR93-3019) are gratefully acknowledged.

- ¹H. C. Andersen, D. Chandler, and J. D. Weeks, *Adv. Chem. Phys.* **34**, 105 (1976).
- ²J. W. E. Lewis and S. W. Lovesey, *J. Phys. C* **10**, 3221 (1977); G. Jacucci and I. R. McDonald, *Mol. Phys.* **39**, 515 (1980).
- ³J. P. Hansen and I. R. McDonald, *Theory of Simple Liquids* (Academic, London, 1986).
- ⁴I. Ebbsjö, T. Kinnel, and I. Waller, *J. Phys. C* **13**, 1865 (1980).
- ⁵M. Canales and J. A. Padró, *Phys. Rev. E* **56**, 1759 (1997).
- ⁶M. Canales and J. A. Padró, *Phys. Rev. E* **60**, 551 (1999).
- ⁷U. Balucani, A. Torcini, and R. Vallauri, *Phys. Rev. B* **47**, 3011 (1993).
- ⁸M. Canales, L. E. González, and J. A. Padró, *Phys. Rev. E* **50**, 3656 (1994).
- ⁹G. Jacucci, M. Ronchetti, and W. Schirmacher, in *Condensed Matter Research Using Neutrons*, edited by S. W. Lovesey and R. Scherm (Plenum, New York, 1984), p. 139.
- ¹⁰J. Bosse, G. Jacucci, M. Ronchetti, and W. Schirmacher, *Phys. Rev. Lett.* **57**, 3277 (1986).
- ¹¹R. Fernández-Perea, M. Alvarez, F. J. Bermejo, P. Verkerk, B. Roessli, and E. Enciso, *Phys. Rev. E* **58**, 4568 (1998), and references therein.
- ¹²U. Balucani and M. Zoppi, *Dynamics of the Liquid State* (Clarendon, Oxford, 1994).
- ¹³S. Kambayashi and Y. Hiwatari, *Phys. Rev. E* **49**, 1251 (1994).
- ¹⁴J. P. Boon and S. Yip, *Molecular Hydrodynamics* (McGraw-Hill, New York, 1980).
- ¹⁵S. D. Wijeyesekera and J. N. Kushick, *J. Chem. Phys.* **71**, 1397 (1979).
- ¹⁶T. Gaskell and S. Miller, *J. Phys. C* **11**, 3749 (1978).
- ¹⁷T. Gaskell and S. Miller, *J. Phys. C* **11**, 4839 (1978).
- ¹⁸U. Balucani, J. P. Brodholt, and R. Vallauri, *J. Phys.: Condens. Matter* **8**, 6139 (1996).
- ¹⁹B. J. Berne and G. D. Harp, *Adv. Chem. Phys.* **17**, 216 (1970).
- ²⁰L. Sjögren and A. Sjölander, *J. Phys. C* **12**, 4369 (1979).
- ²¹M. Canales and J. A. Padró, *J. Phys.: Condens. Matter* **9**, 11009 (1997).
- ²²K. E. Larson, *J. Phys.: Condens. Matter* **6**, 2835 (1994).